2011 IEEE 15th Workshop on Signal Propagation on Interconnects,
May 8-11, 2011, Naples, Italy, pp. 121-124

A Simple Computation of the High-Frequency Per-Unit-Length Resistance Matrix

Frédéric Broydé and Evelyne Clavelier
Tekcem
Maule, France
e-mail: {fredbroyde,eclavelier}@tekcem.com

***Abstract* — Based on multiconductor transmission line (MTL) theory, we determine the relationship between the high-frequency (h.f.) current distribution in a multiconductor interconnection and the electrostatic charge distribution in a lossless interconnection without dielectrics. This result is used to compute the h.f. per-unit-length resistance matrix of the interconnection.**

I. Introduction

We consider a uniform multiconductor interconnection having n transmission conductors (TCs) and a reference conductor also referred to as ground conductor (GC), for instance used for signal transmission in a parallel link. The cross-section of such an $(n+1)$-conductor interconnection is shown in Fig. 1, in the special case of a simple multiconductor microstrip structure. We want to describe the high-frequency (h.f.) current distribution in the cross-section of this “interconnection 1” and to use this result to compute its h.f. per-unit-length (p.u.l.) resistance matrix.

In the case of a two-conductor interconnection (for which $n = 1$), the detailed current distribution is usually computed as the solution of equations involving the longitudinal electric field [1]. In this paper, we consider a different approach which only applies to the h.f. current distribution and is based on the quasi-TEM approximation. However, our approach is easily implemented, even in the case $n \geq 2$. We define an “interconnection 2” as identical to the interconnection 1, except that, in the interconnection 2, the dielectrics are replaced with vacuum and the conductors are replaced with ideal conductors having the same geometry. Section II states some results of electromagnetic theory and multiconductor transmission line (MTL) theory, applicable to the interconnection 2. In Sections III and IV, we establish general properties of the current and charge distributions in the interconnections 1 and 2. In Sections V and VI, these results are used to derive the h.f. current distribution and the h.f. p.u.l. resistance matrix of the interconnection 1.

II. Lossless Interconnection Without Dielectrics

In the interconnection 2, we only consider the propagation of TEM waves along the z axis, which takes place at the velocity of light in vacuum, denoted by c_0. The most general frequency domain electric field solution is given by [2, § 9.1] [3, § 3.1]

$$\mathbf{E} = \mathbf{E}_A(x,y)\, e^{-j\frac{\omega}{c_0}z} + \mathbf{E}_B(x,y)\, e^{+j\frac{\omega}{c_0}z} \tag{1}$$

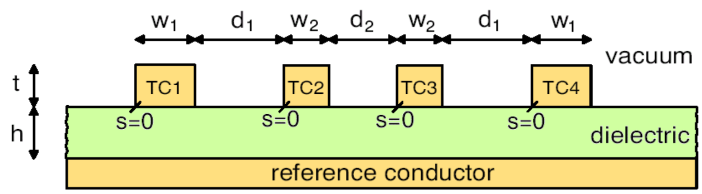

Fig. 1. Cross-section of a multiconductor microstrip interconnection having n = 4 transmission conductors (TCs) and a reference conductor (GC). The arc length on the perimeter of each TC, denoted by s, is explained and used in Section V.

where ω is the radian frequency, $\mathbf{E}_A(x, y)$ is a transverse electric field applicable to a wave propagating in the direction of increasing z, and $\mathbf{E}_B(x, y)$ is a transverse electric field applicable to a wave propagating in the direction of decreasing z. The two-dimensional fields $\mathbf{E}_A(x, y)$ and $\mathbf{E}_B(x, y)$ are related to the two-dimensional gradients of the potential functions $\psi_A(x, y)$ and $\psi_B(x, y)$, by $\mathbf{E}_A(x, y) = -\nabla_T \psi_A(x, y)$ and $\mathbf{E}_B(x, y) = -\nabla_T \psi_B(x, y)$, where ∇_T denotes the transverse part of the vector operator ∇. The magnetic field is given by

$$\mathbf{H} = \frac{1}{\eta_0}\mathbf{e}_z \times \left(\mathbf{E}_A(x,y)\, e^{-j\frac{\omega}{c_0}z} - \mathbf{E}_B(x,y)\, e^{+j\frac{\omega}{c_0}z} \right) \tag{2}$$

where $\mathbf{e}_z$ denotes the unit vector of the z axis and η_0 is the intrinsic impedance of free-space. The equations (1) and (2) are direct consequences of Maxwell’s equations.

According to MTL theory, for any interconnection, the column-vector of the voltages of the TCs with respect to the GC, denoted by $\mathbf{V}(z)$, and the column-vector of the currents on the TCs, denoted by $\mathbf{I}(z)$, are given by [4, § 4.3.2] [5]

$$\mathbf{I}(z) = \mathbf{T}\left(e^{-\Gamma z}\mathbf{T}^{-1}\mathbf{I}_A - e^{+\Gamma z}\mathbf{T}^{-1}\mathbf{I}_B\right) \tag{3}$$

$$\mathbf{V}(z) = \mathbf{Z}_C\mathbf{T}\left(e^{-\Gamma z}\mathbf{T}^{-1}\mathbf{I}_A + e^{+\Gamma z}\mathbf{T}^{-1}\mathbf{I}_B\right) \tag{4}$$

where $\mathbf{T}$ is the transition matrix from modal currents to natural currents, Γ is the diagonal matrix of the propagation constants, $\mathbf{Z}_C$ is the characteristic impedance matrix of the MTL and where $\mathbf{I}_A$ and $\mathbf{I}_B$ are column-vectors of currents determined by the configurations at the ends of the interconnection. For the interconnection 2, $\Gamma = (\omega/c_0)\ \mathbf{1}_n$, where $\mathbf{1}_n$ denotes the identity matrix of size $n \times n$, $\mathbf{Z}_C$ is real and we may choose $\mathbf{T} = \mathbf{1}_n$ [4, § 4.4.1]. Thus, we may write

$$\mathbf{V}(z) = \mathbf{V}_A\, e^{-j\frac{\omega}{c_0}z} + \mathbf{V}_B\, e^{+j\frac{\omega}{c_0}z} \tag{5}$$

$$\mathbf{I}(z) = \mathbf{Z}_C^{-1}\left(\mathbf{V}_A\, e^{-j\frac{\omega}{c_0}z} - \mathbf{V}_B\, e^{+j\frac{\omega}{c_0}z}\right) \tag{6}$$

where $\mathbf{V}_A$ and $\mathbf{V}_B$ are column-vectors of voltages determined by the configurations at the ends of the interconnection. Clearly, $\psi_A(x, y)$ is the solution of Laplace's equation $\nabla_T^{\,2}\psi_A(x, y) = 0$ for the Dirichlet boundary conditions defined by $\mathbf{V}_A$, while $\psi_B(x, y)$ is the solution of Laplace's equation $\nabla_T^{\,2}\psi_B(x, y) = 0$ for the Dirichlet boundary conditions defined by $\mathbf{V}_B$.

III. Surface Current Density

In the interconnection 2, the surface current density being axial (i.e. parallel to $\mathbf{e}_z$), the axial component of the surface current density on the surface of the conductors is given by

$$j_S = \mathbf{e}_z \cdot \left[\mathbf{n} \times \mathbf{H}(x,y,z)\right] \tag{7}$$

where $\mathbf{n}$ is the unit vector normal to the boundary drawn from the conductor to vacuum. Using (2), we get

$$j_S = \frac{\mathbf{n}}{\eta_0} \cdot \left[\mathbf{E}_A(x,y)\, e^{-j\frac{\omega}{c_0}z} - \mathbf{E}_B(x,y)\, e^{+j\frac{\omega}{c_0}z}\right] \tag{8}$$

Let us consider a first configuration where, at a given abscissa $z = z_G$, a column-vector of the currents on the conductors, denoted by $\mathbf{I}(z_G)$, is observed. On the boundary of the conductors, according to (8), we may write

$$j_S = \frac{\mathbf{n}}{\eta_0} \cdot \mathbf{E}_G(x,y) = -\frac{\mathbf{n}}{\eta_0} \cdot \nabla_T \psi_G(x,y) \tag{9}$$

where

$$\mathbf{E}_G(x,y) = \mathbf{E}_A(x,y)\, e^{-j\frac{\omega}{c_0}z_G} - \mathbf{E}_B(x,y)\, e^{+j\frac{\omega}{c_0}z_G} \tag{10}$$

and

$$\psi_G(x,y) = \psi_A(x,y)\, e^{-j\frac{\omega}{c_0}z_G} - \psi_B(x,y)\, e^{+j\frac{\omega}{c_0}z_G} \tag{11}$$

Here, $\psi_G(x, y)$ is the solution of Laplace's equation $\nabla_T^{\,2}\psi_G(x, y) = 0$ for the Dirichlet boundary conditions defined by

$$\mathbf{V}_A\, e^{-j\frac{\omega}{c_0}z_G} - \mathbf{V}_B\, e^{+j\frac{\omega}{c_0}z_G} = \mathbf{Z}_C \mathbf{I}(z_G) \tag{12}$$

where we have used (6). Consequently, the surface current density j_S does not depend on the choice of $\mathbf{V}_A$ and $\mathbf{V}_B$ and is uniquely defined by $\mathbf{I}(z_G)$. Clearly, $\psi_G(x, y)$ is a linear function of $\mathbf{I}(z_G)$, but it is otherwise independent of z_G and of frequency. Consequently, at a given (x, y) on the boundary of the conductors at $z = z_G$, using (9), we find that j_S is a linear function of $\mathbf{I}(z_G)$, which may be represented with the matrix $\mathbf{M}(x, y)$ such that

$$j_S(x,y,z_G) = \mathbf{M}(x,y)\, \mathbf{I}(z_G) \tag{13}$$

where $\mathbf{M}(x, y)$ is frequency-independent and has the dimensions of m^{-1}. Moreover, we observe that, if $\mathbf{I}(z_G)$ is a real vector, $\psi_G(x, y)$ is a real potential function because, in (12), $\mathbf{Z}_C$ is a real matrix. Thus, if $\mathbf{I}(z_G)$ is a real vector, (9) shows that j_S is real, so that $\mathbf{M}(x, y)$ is real.

For the interconnection 1, our reasoning does not apply because (2) and (6) need not be satisfied. Let us assume that resistive losses are small, so that the currents mainly flow close to the surface of the conductors and a surface current density j_S can be considered. No general formula can be used in place of (8) since MTL theory is exactly compatible with Maxwell equations only in the case of an homogeneous medium surrounding perfect conductors. However, in the framework of MTL theory, at each abscissa z, the effects of $\mathbf{I}(z)$, such as the magnetic field and the resulting j_S given by (7), are assumed to be independent from the effects of $\mathbf{V}(z)$, such as the electric field, so that j_S is unaffected by the presence of dielectrics. Thus, we can state the following theorem.

Theorem on the surface current density. At a given abscissa $z = z_G$ of the interconnection 1, for small resistive losses (h.f. current distribution), the surface current density j_S on the boundary of the conductors is given by (13), where $\mathbf{M}(x, y)$ is a real $1 \times n$ matrix which neither depends on the abscissa nor on the frequency.

IV. Surface Charge Density

In the interconnection 2, at the boundary of the conductors, the surface charge density is given by

$$\rho_S = \varepsilon_0\, \mathbf{n} \cdot \left[\mathbf{E}_A(x,y)\, e^{-j\frac{\omega}{c_0}z} + \mathbf{E}_B(x,y)\, e^{+j\frac{\omega}{c_0}z}\right] \tag{14}$$

where ε_0 is the permittivity of vacuum. Let us consider a second configuration where, at an abscissa $z = z_H$, a column-vector of the p.u.l. charge density on the boundary of the conductors, denoted by $\mathbf{Q}(z_H)$, is observed. By charge conservation, we have

$$j\omega\, \mathbf{Q}(z_H) = -\left.\frac{d\,\mathbf{I}}{dz}\right|_{z_H} \tag{15}$$

Using (5) and (6), we get

$$\mathbf{Q}(z_H) = \frac{\mathbf{Z}_C^{-1}}{c_0}\left(\mathbf{V}_A\, e^{-j\frac{\omega}{c_0}z_H} + \mathbf{V}_B\, e^{+j\frac{\omega}{c_0}z_H}\right) = \frac{\mathbf{Z}_C^{-1}\mathbf{V}(z_H)}{c_0} \tag{16}$$

At $z = z_H$, on the boundary of the conductors, according to (14), we may write

$$\rho_S = \varepsilon_0\, \mathbf{n} \cdot \mathbf{E}_H = -\varepsilon_0\, \mathbf{n} \cdot \nabla_T \psi_H \tag{17}$$

where

$$\mathbf{E}_H(x,y) = \mathbf{E}_A(x,y)\, e^{-j\frac{\omega}{c_0}z_H} + \mathbf{E}_B(x,y)\, e^{+j\frac{\omega}{c_0}z_H} \tag{18}$$

and

$$\psi_H(x,y) = \psi_A(x,y)\, e^{-j\frac{\omega}{c_0}z_H} + \psi_B(x,y)\, e^{+j\frac{\omega}{c_0}z_H} \tag{19}$$

Here, $\psi_H(x, y)$ is the solution of Laplace's equation $\nabla_T^{\,2}\psi_H(x, y) = 0$ for the Dirichlet boundary conditions defined by

$$\mathbf{V}_A\, e^{-j\frac{\omega}{c_0}z_H} + \mathbf{V}_B\, e^{+j\frac{\omega}{c_0}z_H} = \mathbf{V}(z_H) = c_0\, \mathbf{Z}_C \mathbf{Q}(z_H) \tag{20}$$

where we have used (16). Thus, the surface charge density ρ_S is uniquely defined by $\mathbf{V}(z_H)$ or equivalently by $\mathbf{Q}(z_H)$. We see that

$\psi_H(x, y)$ is a linear function of $\mathbf{Q}(z_H)$, but it is otherwise independent of z_H and of the frequency. Consequently, at a given (x, y) on the boundary of the conductors at $z = z_H$, ρ_S is a linear function of $\mathbf{Q}(z_H)$, which may be represented with the frequency-independent matrix $\mathbf{N}(x, y)$ such that

$$\rho_S(x, y, z_H) = \mathbf{N}(x, y)\,\mathbf{Q}(z_H) \tag{21}$$

where $\mathbf{N}(x, y)$ has the dimensions of m^{-1}. Additionally, we observe that, if $\mathbf{Q}(z_H)$ is a real vector, $\psi_H(x, y)$ and $\mathbf{V}(z_H)$ are real because $\mathbf{Z}_C$ is a real matrix. Thus, if $\mathbf{Q}(z_H)$ is real, (17) shows that ρ_S is real, so that $\mathbf{N}(x, y)$ is real and describes the electrostatic charge distribution. We have proved a second theorem.

Theorem on the surface charge density. At a given abscissa $z = z_H$ of the interconnection 2, the surface charge density ρ_S on the boundary of the conductors is given by (21), where $\mathbf{N}(x, y)$ is a real $1 \times n$ matrix which neither depends on the abscissa nor on the frequency, $\mathbf{N}(x, y)$ describing the electrostatic charge distribution.

V. High-Frequency Current Distribution

We now observe that $\psi_G(x, y)$ and $\psi_H(x, y)$ are the solutions of Laplace's equation for the Dirichlet boundary conditions defined by $\mathbf{Z}_C\ \mathbf{I}(z_G)$ and $c_0\ \mathbf{Z}_C\ \mathbf{Q}(z_H)$, respectively. Thus, for $\mathbf{I}(z_G) = c_0\ \mathbf{Q}(z_H)$ we have $\psi_G(x, y) = \psi_H(x, y)$, so that (9) and (17) show that $\rho_S / \varepsilon_0 = \eta_0\, j_S$. Consequently,

$$\mathbf{N}(x, y) = \mathbf{M}(x, y) \tag{22}$$

Thus, we obtain the following theorem.

Theorem on the connection of charge and current densities. For an MTL with small resistive losses (h.f. current distribution), at a given abscissa z, for a given $\mathbf{I}(z)$, the surface current density j_S at the surface of the conductors is the product of an arbitrary velocity v_D and the surface charge density at the surface of the conductors in a configuration where all dielectrics are replaced by vacuum and where $\mathbf{Q}(z) = \mathbf{I}(z)/v_D$.

Let us now see how this theorem can be used to easily determine the h.f. current distribution. The MTL model of the interconnection includes the h.f. p.u.l. external inductance matrix of the interconnection 1, denoted by $\mathbf{L}_0$ and often referred to as the p.u.l. external inductance matrix. This matrix is given by $\mathbf{L}_0 = \mu_0\,\varepsilon_0\,\mathbf{C}_0^{-1}$, where μ_0 is the permeability of vacuum and $\mathbf{C}_0$ is the p.u.l. capacitance matrix of the interconnection 2, as shown by Pipes [6, § IV.3]. In order to assess $\mathbf{C}_0$, the perimeter of each TC is usually divided in small strips. Let us use A to denote the set of the indices of the strips which form the boundaries of all TCs. The set A may be partitioned into mutually exclusive subsets $A_1, \ldots A_n$, where for any integer j such that $1 \le j \le n$, the subset A_j contains the indices of the strips of the TC number j. At the final stage of the computation of $\mathbf{C}_0$ by the method of moment using pulse expansion and point matching [4, § 3.3], a capacitance matrix $\mathcal{C}_0$ is computed, an entry $\mathcal{C}_{0\,\alpha\beta}$ of $\mathcal{C}_0$ being the p.u.l. charge of the strip number α when the voltage between the center of the strip number β and ground is 1 V, the voltage between the center of each other strip and ground being 0 V. The entry $C_{0\,ij}$ of $\mathbf{C}_0$ is given by

$$C_{0\,ij} = \sum_{\alpha \in A_i} \sum_{\beta \in A_j} \mathcal{C}_{0\,\alpha\beta} \tag{23}$$

At this point, an estimate of $\mathbf{N}(x, y) = \mathbf{M}(x, y)$ is available, since, at any point (X, Y) on the strip number α we have

$$\mathbf{N}(X, Y) \approx \frac{1}{w_\alpha} \sum_{j=1}^{n} \left(\sum_{\beta \in A_j} \mathcal{C}_{0\,\alpha\beta} \right) {}^{t}\mathbf{e}_j\,\mathbf{C}_0^{-1} \tag{24}$$

where we use w_α to denote the width of the strip α, where ${}^{t}\mathbf{A}$ denotes the transpose of $\mathbf{A}$ and where $\mathbf{e}_j$ denotes the column-vector having n entries, said entries being zero except the j-th entry which is equal to 1. Let us for instance consider the interconnection shown in Fig. 1, with $t = w_1 = w_2 = 50$ µm and $h = d_1 = d_2 = 50$ µm. On a given TC, the normalized arc length along the perimeter of the cross section increases clockwise, from the point $s = 0$, shown in Fig. 1, to $s = 1$. The Fig. 2 shows the current distribution on the TCs when a current is injected on a single TC, computed using (24) and 336 matching points. Current crowding is visible near edges. The proximity effect is also plain. Thus, eddy currents are induced in all non-excited conductors, and this phenomenon will contribute to the h.f. resistive losses.

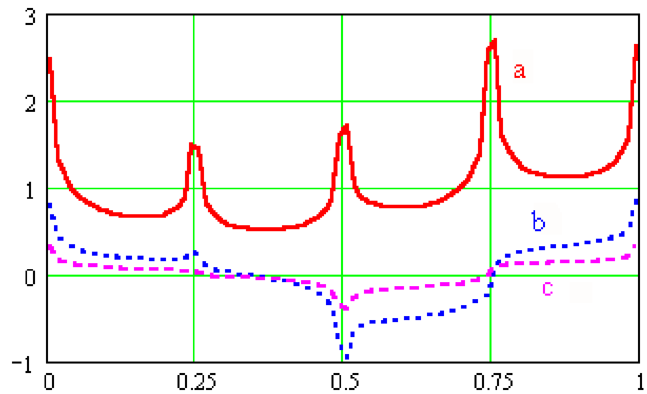

Fig. 2. Surface current density (arbitrary unit) measured on TC 1, versus s, when a current is injected in the TC 1 (a), TC 2 (b) or TC 3 (c).

VI. High-Frequency P.U.L. Resistance Matrix

Let us assume that we inject the currents of the column-vector $\mathbf{I}$ into the TCs. Let us use $i_S(\alpha, \mathbf{I})$ to denote the current flowing in the strip α. For any j, we have

$$\sum_{\alpha \in A_j} i_S(\alpha, \mathbf{I}) = [\mathbf{I}]_j \tag{25}$$

where $[\mathbf{x}]_j$ is the j-th entry of the vector $\mathbf{x}$. At high frequencies, according to the theorem on the surface current density, we may define a real matrix $\mathbf{Q}_V$ having n columns such that, for any $\mathbf{I}$, the current flowing in the strip α is given by

$$i_S(\alpha, \mathbf{I}) = k\,[\mathbf{Q}_V\ \mathbf{I}]_\alpha \tag{26}$$

where k is an arbitrary non-zero constant. Using (25), we get

$$i_S(\alpha, \mathbf{I}) = \sum_{j=1}^{n} \frac{Q_{V\,\alpha\,j} I_j}{\sum_{\beta \in A_j} Q_{V\,\beta\,j}} \tag{27}$$

where the $Q_{V\,\alpha\,j}$ are the entries of $\mathbf{Q}_V$. Let us assume that the resistivity and the skin depth are the same in all TCs and denoted by ρ_{TC} and δ_{TC}, respectively. At sufficiently high frequencies, the thickness and width of each TC are each much greater than δ_{TC}. The surface current density being homogeneous over each strip, the p.u.l. power dissipated in the TCs is

$$P_{TC} = \frac{\rho_{TC}}{\delta_{TC}} \sum_{\alpha \in A} \frac{\left| i_S(\alpha, \mathbf{I}) \right|^2}{w_\alpha} \tag{28}$$

The h.f. p.u.l. resistance matrix of the TCs, denoted by $\mathbf{R}_{HFTC}$, is defined by $P_{TC} = \mathbf{I}^* \, \mathbf{R}_{HFTC} \, \mathbf{I}$, where $\mathbf{I}^*$ denotes the hermitian adjoint of $\mathbf{I}$. Using (27) and (28), we may easily show that

$$\mathbf{R}_{HFTC} = \frac{\rho_{TC}}{\delta_{TC}} \mathbf{K}_{TC} \tag{29}$$

where we refer to $\mathbf{K}_{TC}$ as the matrix of the equivalent inverse widths of the TCs, the entries of $\mathbf{K}_{TC}$ being given by

$$K_{TC\,i\,j} = \frac{1}{\left(\sum_{\beta \in A_i} Q_{V\,\beta\,i} \right) \left(\sum_{\beta \in A_j} Q_{V\,\beta\,j} \right)} \sum_{\alpha \in A} \frac{Q_{V\,\alpha\,i} Q_{V\,\alpha\,j}}{w_\alpha} \tag{30}$$

At this stage, the theorem on the connection of charge and current densities can be used to obtain $\mathbf{Q}_V$, since it tells us that we may define $Q_{V\,\alpha\,i}$ as the p.u.l. electrostatic charge on the strip α when the p.u.l charge of the TC number i is 1, the p.u.l. charge on each other TC being zero. In other words, we can use

$$Q_{V\,\alpha\,i} = \sum_{j=1}^{n} \left(\sum_{\beta \in A_j} c_{0\,\alpha\,\beta} \right) {}^t\mathbf{e}_j \mathbf{C}_0^{-1} \mathbf{e}_i \tag{31}$$

A similar reasoning can be used to obtain the h.f. p.u.l. resistance matrix of the GC, denoted by $\mathbf{R}_{HFGC}$, defined by $P_{GC} = \mathbf{I}^* \, \mathbf{R}_{HFGC} \, \mathbf{I}$, where P_{GC} is the p.u.l. power dissipated in the GC. Using ρ_{GC} and δ_{GC} to denote the resistivity and the skin depth of the GC, respectively, we find

$$\mathbf{R}_{HFGC} = \frac{\rho_{RC}}{\delta_{RC}} \mathbf{K}_{GC} \tag{32}$$

where we refer to $\mathbf{K}_{GC}$ as the matrix of the equivalent inverse widths of the GC, the entries of $\mathbf{K}_{GC}$ being given by

$$K_{GC\,i\,j} = \frac{\int_C \{\mathbf{n} \cdot \mathbf{E}_i(\xi)\} \{\mathbf{n} \cdot \mathbf{E}_j(\xi)\} \, d\xi}{\left(\int_C \mathbf{n} \cdot \mathbf{E}_i(\xi) \, d\xi \right) \left(\int_C \mathbf{n} \cdot \mathbf{E}_j(\xi) \, d\xi \right)} \tag{33}$$

where ξ is an arc length on the boundary of the GC and where $\mathbf{E}_i(\xi)$ is the electrostatic field component normal to the surface of the GC when the p.u.l. charge of each strip is given by (31), the integration path C extending over the boundary of the GC.

Finally, the h.f. resistance matrix of the interconnection, denoted by $\mathbf{R}_{HF}$, is given by

$$\mathbf{R}_{HF} = \mathbf{R}_{HFTC} + \mathbf{R}_{HFGC} = \frac{\rho_{TC}}{\delta_{TC}} \mathbf{K}_{TC} + \frac{\rho_{GC}}{\delta_{GC}} \mathbf{K}_{GC} \tag{34}$$

The conductors being reciprocal and passive, $\mathbf{K}_{TC}$ and $\mathbf{K}_{GC}$ are frequency-independent real positive semidefinite matrices [7, § 7.1]. Thus, any diagonal entry of $\mathbf{K}_{TC}$ or $\mathbf{K}_{GC}$ is non-negative. As an example, for the multiconductor microstrip interconnection considered in Section V, using 336 matching points,$\mathbf{K}_{TC}$ and $\mathbf{K}_{GC}$ given by (30), (31) and (33) are:

$$\mathbf{K}_{TC} = \begin{pmatrix} 6961 & 806 & 88 & 0 \\ 806 & 7466 & 985 & 88 \\ 88 & 985 & 7466 & 806 \\ 0 & 88 & 806 & 6961 \end{pmatrix} \mathrm{m}^{-1} \tag{35}$$

and

$$\mathbf{K}_{GC} = \begin{pmatrix} 2238 & 1622 & 951 & 563 \\ 1622 & 2157 & 1582 & 951 \\ 951 & 1582 & 2157 & 1622 \\ 563 & 951 & 1622 & 2238 \end{pmatrix} \mathrm{m}^{-1} \tag{36}$$

We have computed $\mathbf{K}_{TC}$ and $\mathbf{K}_{GC}$ in many different configurations. Note that a non-diagonal entry of $\mathbf{K}_{TC}$ is not always positive. We always found that $\mathbf{K}_{TC}$ is strictly diagonally dominant [7, § 6.1.9], and that $\mathbf{K}_{GC}$ is nonnegative [7, § 8.1].

VII. Conclusion

We have determined general properties of the h.f. current distribution in a multiconductor interconnection, in particular its connection with the electrostatic charge distribution in the interconnection when the dielectrics are removed. These properties can be used to assess $\mathbf{R}_{HF}$ based on an approximation which takes into account the crowding of currents at the edges of a conductor (edge effect), and the influence of other conductors (proximity effect). This approach does not require a large computational effort after the computation of $\mathbf{L}_0$. In the case where the TCs have the same homogeneous resistivity, it is convenient to use the frequency-independent $\mathbf{K}_{TC}$ and $\mathbf{K}_{GC}$ to obtain the frequency-dependent $\mathbf{R}_{HFTC}$ and $\mathbf{R}_{HFGC}$ as a function of frequency.

References

[1] A. Cangellaris, "A Note on the calculation of the current distribution in lossy microstrip structures", *IEEE Microwave Guided Wave Lett.*, Vol. 1, No. 4, April 1991, pp. 81-83.

[2] C.T.A. Johnk, *Engineering Electromagnetic Fields and Waves*, John Wiley & Sons, 1975.

[3] R.E. Collin, *Field Theory of Guided Waves*, 2nd ed., IEEE Press, 1991.

[4] C.R. Paul, *Analysis of Multiconductor Transmission Lines*, John Wiley & Sons, 1994.

[5] F. Broydé, E. Clavelier, "A new method for the reduction of crosstalk and echo in multiconductor interconnections", *IEEE Trans. Circuits Syst. I*, vol. 52, No. 2, pp. 405-416, Feb. 2005.

[6] L.A. Pipes, "Steady-State Analysis of Multiconductor Transmission Lines", *Journal of Applied Physics*, vol. 12, November 1941, pp. 782-799.

[7] R.A. Horn, C.R. Johnson, *Matrix analysis*, Cambridge University Press, 1985.